Journal of Orthopaedic Translation 49 (2024) 207–217

Contents lists available at ScienceDirect

Journal of Orthopaedic Translation

journal homepage: www.journals.elsevier.com/journal-of-orthopaedic-translation

Original Article

IHH–GLI-1–HIF-2α signalling influences hypertrophic chondrocytes to exacerbate osteoarthritis progression

Chengming Zhang [a], Ruipeng Zhao [a], Zhengquan Dong [a], Yang Liu [b], Mengrou Liu [a], Haoqian Li [a], Yukun Yin [a], Xianda Che [a], Gaige Wu [a], li Guo [a], Pengcui Li [a,**], Xiaochun Wei [a,*], Ziquan Yang [c,***]

[a] Shanxi Key Laboratory of Bone and Soft Tissue Injury Repair, Department of Orthopedics, Second Hospital of Shanxi Medical University, Taiyuan, 030001, PR China
[b] Department of Laboratory Medicine, Handan Second Hospital, Hebei University of Engineering, Handan, 056000, PR China
[c] Department of Orthopedics, First Hospital of Shanxi Medical University, Taiyuan, 030000, PR China

ARTICLE INFO

Keywords:
Chondrocyte hypertrophy
GLI proteins
HIF-2α
Indian hedgehog
Osteoarthritis

ABSTRACT

Background: Chondrocyte hypertrophy is a potential target for osteoarthritis (OA) treatment, with Indian hedgehog (IHH), glioma-associated oncogene homolog (GLI), and hypoxia-inducible factor-2α (HIF-2α) being closely associated with chondrocyte hypertrophy during OA progression. Whereas IHH can modulate chondrocyte hypertrophy, interference with IHH signalling has not achieved the anticipated therapeutic effects and poses safety concerns, necessitating further clarification of the specific mechanisms by which IHH affects articular cartilage degeneration. Inhibition of the HIF-2α overexpression in cartilage slows the progression of early OA, but the mechanisms underlying HIF-2α accumulation in OA cartilage remain unclear. The aim of this study was to determine the function of Ihh, as well as its downstream factors, in chondrocytes, based on an early osteoarthritis (OA) mouse model and in vitro chondrocyte model.

Methods: Investigated the expression levels and locations of IHH–GLI-1 pathway in normal and early degenerated human cartilage, comparing them with HIF-2α and its downstream factors. RT-qPCR, Western blotting, Crystal violet staining, and EdU assays were used to evaluate the pecific regulatory mechanisms of the IHH–GLI-1–HIF-2α signalling axis in normal chondrocytes and in chondrocytes under inflammatory conditions. Validated the impact of IHH on early cartilage degeneration and the relationship between the IHH-GLI-1 pathway and the expression levels and expression locations of HIF-2α and its downstream factors in Col2a1-Cre^{ERT2};Ihh$^{fl/fl}$ mice.

Results: In early-stage degenerative joint cartilage, the GLI-1 pathway in hypertrophic chondrocytes exhibited similar changes in location and levels to HIF-2α and its downstream factor vascular endothelial growth factor (VEGF). In vitro, IHH–GLI-1–HIF-2α signalling activation in chondrocytes under physiological hypoxic conditions inhibited chondrocyte proliferation. In chondrocytes stimulated by inflammatory environments, IHH inhibited the degradation of HIF-2α via the GLI-1 pathway, thereby promoting HIF-2α protein expression. Elevated HIF-2α expression further enhanced intracellular IHH–GLI-1 levels, generating a positive feedback loop to collectively regulate the expression of downstream hypertrophic factors and matrix-degradation factors. *In vivo*, conditional *Ihh* knockout in mouse chondrocytes downregulated Hif-2α protein expression in early degenerative cartilage tissue and affected the expression of downstream Vegf and hypertrophic factors.

Conclusions: During OA progression, the IHH–GLI-1–HIF-2α axis mainly operates within hypertrophic chondrocytes, exacerbating cartilage degeneration by regulating hypertrophic chondrocyte functions, cartilage matrix degradation, and microvascular invasion.

The translational potential of this article: This study identifies the IHH-GLI-1-HIF-2α signalling axis and reveals its potential as a therapeutic target for OA.

* Corresponding author.
** Corresponding author.
*** Corresponding author.
E-mail addresses: lpc1977@163.com (P. Li), sdeygksys@163.com (X. Wei), yzqonline@126.com (Z. Yang).

https://doi.org/10.1016/j.jot.2024.09.008
Received 16 June 2024; Received in revised form 9 September 2024; Accepted 25 September 2024

1. Introduction

Osteoarthritis (OA), a chronic, incurable joint ailment chiefly characterised by progressive articular cartilage deterioration, significantly contributes to pain and disability among the aging populace [1]. The primary mechanism triggering cartilage degeneration involves chondrocyte transition into a state of hypertrophic proliferation within the cartilage, marked by abnormal hypertrophic differentiation, ultimately leading to extracellular matrix (ECM) breakdown [2]. Chondrocytes, the sole occupants of healthy cartilage, maintain cartilage homeostasis [3]. Chondrocyte hypertrophy, characterised by increases in size, volume, and collagen type X (COL-X) and matrix metalloproteinase 13 (MMP13) expression and marking terminal differentiation of these cells, is pivotal for endochondral ossification and skeletal development [4,5]. Whereas chondrocyte hypertrophy is crucial for skeletal growth and development, it becomes detrimental during cartilage degeneration. Numerous studies have provided evidence of chondrocyte hypertrophy during cartilage destruction, emphasising its significance for OA progression [6,7]. Throughout chondrocyte hypertrophy, numerous metalloproteinases are synthesised, alongside the secretion of hypertrophic factors, such as Indian hedgehog (IHH), hypoxia-inducible factor-2α (HIF-2α), runt-related transcription factor 2, and vascular endothelial growth factor (VEGF), exacerbating differentiation [6,8–11]. These factors mediate continuous degradation of the cartilage matrix, impeding repair, and ultimately culminating in the loss of a stable articular cartilage structure, exacerbating OA progression [12].

During chondrocyte hypertrophy and differentiation, IHH assumes a central role. As a hedgehog protein family member, it governs chondrocyte proliferation, hypertrophic differentiation, and osteogenic differentiation [13]. Its effects on cartilage and bone development primarily occur via the glioma-associated oncogene homolog (GLI) pathway and a parathyroid hormone-related protein (PTHrP) negative feedback mechanism [13], with IHH significantly associated with articular cartilage degeneration [14,15]. Modulating IHH activity or downstream signalling in articular cartilage modifies OA progression [16–19]. Additionally, downstream of IHH signalling, GLI-1 influences OA progression [16,20]. Consequently, inhibiting IHH signalling has emerged as a plausible strategy for OA prevention or treatment. However, comprehensive interference with the entire IHH pathway could yield complex effects, potentially thwarting anticipated therapeutic outcomes and prompting safety concerns [21]. Therefore, further research to elucidate the specific mechanisms through which IHH affects articular cartilage degeneration is imperative.

Cartilage matrix degradation, a hallmark of articular cartilage degeneration, is directly induced by various catabolic factors, such as interleukin-1β (IL-1β), tumour necrosis factor-α (TNF-α), and MMPs [22,23]; these are regulated by HIF-2α [24], which is closely associated with chondrocyte hypertrophy [10]. Consequently, HIF-2α is a major mediator of and potential therapeutic target for OA [25]. HIF-2α accumulates in naturally hypoxic cartilage tissue [26], and its expression increases as OA progresses, suggesting complex regulatory mechanisms [25]. This accumulation could result from multifactorial regulation including oxygen levels and inflammation. As a crucial OA regulator, understanding its accumulation mechanism during cartilage degeneration and selectively inhibiting its expression could alleviate early OA progression. In hepatocellular carcinoma tissues, Hedgehog signalling might induce HIF-1α degradation via the RACK1–HSP-90 pathway, thereby affecting vascular generation mediated by the HIF–VEGF axis [27]. Satio found that HIF-2α overexpression in growth-plate chondrocytes can enhance *Ihh* gene expression [10], suggesting potential molecular crosstalk between HIF-2α and IHH in chondrocytes, although the precise underlying mechanism remains unclear. Together, regulating chondrocyte hypertrophic differentiation has emerged as an effective strategy to delay cartilage degeneration. However, the mechanism regulating chondrocyte hypertrophy during cartilage degeneration remains poorly understood. Further clarification of the molecular interactions involved in this process is needed to delay OA progression.

Given the possible correlation between IHH and HIF-2α during cartilage degeneration, we examined alterations in the IHH–GLI-1 pathway and HIF-2α during early human articular cartilage degeneration. Subsequently, we constructed an early-OA model using conditional knockout mice (Col2a1-Cre^{ERT2};Ihh$^{fl/fl}$), inducing the conditional deletion of *Ihh* in chondrocytes using tamoxifen (TM) [28,29], to investigate the effect on HIF-2α and downstream hypertrophic factors in early-OA chondrocytes. We also overexpressed and knocked out *Ihh* in chondrocytes cultured under hypoxic conditions and simulated arthritis environments to elucidate the roles of IHH and HIF-2α in cartilage degeneration and clarify the mechanism of HIF-2α accumulation during early cartilage degeneration. Our aim was to identify new targets to delay OA progression.

2. Materials and methods

2.1. Collection of human tibial plateau cartilage tissue

Human cartilage tissue samples were collected from the tibial plateaus of individuals who underwent knee replacement surgery at the Second Hospital of Shanxi Medical University, with KL grade of 3. Cartilage samples from the tibia obtained during total knee arthroplasty were divided into two categories: OA cartilage from the more affected compartment (usually medial); “relatively normal” and “early degenerative” cartilage from the uninvolved compartment (usually lateral). All participants provided written informed consent for inclusion. Research procedures were conducted in strict adherence to the guidelines established by the Ethics Committee of the Second Hospital of Shanxi Medical University (Approval No. 2022. YX.No.167). The work described has been carried out in accordance with The Code of Ethics of the World Medical Association (Declaration of Helsinki) for experiments involving humans.

2.2. Histology, IHC, and Osteoarthritis Research Society International (OARSI) scoring

Cartilage tissue specimens were routinely fixed, decalcified, dehydrated, and embedded in paraffin. Serial sections (5 μm) were cut and stained with 0.2 % Fast Green (Sigma, USA) and 1 % Alcian Blue (Sigma, USA) for cartilage visualisation. For immunohistochemical staining the following antibodies were used: rabbit anti-IHH (Abcam, 1:100), rabbit anti-GLI-1 (ABclonal, 1:200), rabbit anti-PTCH-1 (ABclonal, 1:200), rabbit anti-SMO (Proteintech, 1:100), rabbit anti-HIF-2α (Proteintech, 1:100), rabbit anti-VEGF (Proteintech, 1:100), and rabbit anti-COL-X (Abcam, 1:50).

Human articular cartilage tissue was assessed by three independent researchers using the Mankin scoring system. Scores of 0–1 indicated relatively normal cartilage (n = 6), whereas scores of 2–6 were indicative of early degenerative changes (n = 6) [30]. Three independent researchers employed the OARSI grading system to evaluate mouse Safranin O-fast green-stained sections [31]. Quantitative analysis of immunohistochemical staining results was conducted using ImageJ software (version 1.53k).

2.3. Chondrocyte culture, in vitro hypoxic conditions, and simulation of arthritic environments

ATDC5 cells were obtained from the Cell Bank of the Chinese Academy of Sciences (Shanghai, China). DMEM/F12 was supplemented with 10 % FBS, 100 U/ml penicillin, and 0.1 mg/ml streptomycin (Solarbio Co., Ltd.) to prepare the complete culture medium. All cells utilised were in the logarithmic growth phase.

For hypoxic cell culture, Anaerocult boxes and sachets were procured from Mitsubishi MGC Co., Ltd. (Tokyo, Japan). The oxygen concentration in the Anaerocult Box was maintained at 5 %. Following GFP-Ihh

and si-Ihh transfection for 24 h, cells were transferred to the Anaerocult box for 48 h before subsequent experiments.

To establish an inflammatory chondrocyte culture environment, chondrocytes were seeded in six-well plates at 80–90 % confluence. After entering the logarithmic growth phase, cells were transfected with GFP-Ihh and si-Ihh. After 24 h, the medium was refreshed, and IL-β recombinant protein was added at a final concentration of 20 μmol/ml. Drug intervention commenced 12 h later, and cells were collected for follow-up experiments 48 h after that.

2.4. GFP-Ihh plasmid and si-Ihh transfection

Chondrocytes were seeded in six-well plates at 70–80 % confluence. After entering the logarithmic growth phase, cells were transfected in complete culture medium using jetPRIME transfection reagent with 2 μg of GFP-Ihh plasmid and 2 μg of si-Ihh. Additionally, equivalent amounts of negative control GFP plasmid and siRNA were transfected. After 24 h, the culture medium was refreshed, and successful GFP-Ihh transfection was confirmed via fluorescence microscopy based on green fluorescence. The GFP-Ihh plasmid and si-Ihh were purchased from Genechem (China), with their sequences listed in Supplementary Table S1.

2.5. Crystal violet, EdU, and IHC staining

Chondrocytes were fixed with paraformaldehyde and stained with 0.1 % crystal violet dye for 15 min in the dark. Subsequently, cells were washed, and images were captured using a digital slide scanner (3DHISTECH, Hungary). To assess proliferation, chondrocytes were treated accordingly and evaluated using an EdU staining kit (RiboBio), following the manufacturer's instructions. Images of stained cells were acquired using a digital slide scanner, and positively stained cells were enumerated in three random fields. The proliferation index was calculated as the percentage of EdU-positive cells relative to the number of Hoechst 33,342-stained cells.

Chondrocytes were fixed with paraformaldehyde and labelled with a rabbit anti-HIF-2α antibody (Proteintech, 1:100) to mark HIF-2α. Subsequently, secondary antibodies corresponding to the primary antibodies were used for labelling, and DAPI staining was applied to visualise cell nuclei. Images were acquired using a digital slide scanner.

2.6. PT2385, Gant61, and CHX treatment

After transfecting chondrocytes with GFP-Ihh, the complete culture medium was replaced, and IL-β recombinant protein (20 μmol/ml) was added. Drug intervention began 12 h later. Subsequently, PT2385 (MCE) and GANT61 (MCE) were added to the medium at 20 and 100 μM, respectively, to inhibit HIF-2α and GLI-1 expression. Cell proteins were extracted 24 h after drug loading to the expression levels. Following respective treatments, chondrocytes were treated with 100 μg/ml of CHX (MCE) in the culture medium. Total cell protein was then extracted at 20, 40, and 60 min post-treatment, and western blotting was performed to quantitatively measure target protein expression at different.

2.7. RT-qPCR

Chondrocytes were seeded into a six-well plate and treated. Next, 1 ml of TRIzol reagent was added, and cells were incubated on ice for 15 min to extract total cellular RNA. Mouse cartilage tissue was ground into powder under dry ice, and 1 ml of TRIzol reagent was added to extract total cellular RNA. Subsequently, 20 μl of PrimeScriptTM RT Master Mix reagent was added to perform reverse transcription and synthesise cDNA from the extracted RNA. The resulting cDNA was then subjected to two-step PCR amplification. Relative gene expression was quantified using the $2^{\hat{}(-\Delta\Delta Ct)}$ method. Primer sequences are shown in Supplementary Table S2.

2.8. Western blotting

Chondrocytes were lysed to obtain total protein, and the protein concentration was determined using a BCA assay kit. Equal protein amounts from each group were subjected to 10 % sodium dodecyl sulphate-polyacrylamide gel electrophoresis under reducing conditions. After electrophoresis, the proteins were transferred onto nitrocellulose membranes. The target protein was detected using the corresponding primary antibody, followed by secondary antibody labelling to enhance specificity. Subsequently, the membrane was treated with a highly sensitive electrochemiluminescence detection reagent, allowing the protein bands to emit light, which was captured using a gel imaging system (Bio-Rad Laboratories Co., Ltd.). Target protein expression levels were quantified by analysing the grayscale values of each band using ImageLab software (version 6.0.1, Bio-Rad Laboratories Co., Ltd.).

2.9. Animals

Col2a1-Cre^{ERT2};Ihh$^{fl/fl}$ mice (supplied by WL) were bred as described [28,29]. Mouse genotyping was conducted using conventional PCR, followed by horizontal strip electrophoresis to assess and select suitable transgenic offspring. Genotyping primer sequences are shown in Supplementary Table S3. At 2 months of age, male Col2a1Cre^{ERT2};Ihh$^{fl/fl}$ mice (n = 24) were stratified into two groups, the TM (n = 12) and non-TM (n = 12) groups. Within each group, animals were further subdivided into two subgroups, the DMM (n = 6) and sham (n = 6) groups. In the TM group, 2-month-old mice were administered TM (1 mg/10 g/day, for 5 consecutive days) to induce *Ihh* deletion. Mice in the non-TM group received an equivalent volume of corn oil as a control. At 3 months of age, animals were randomly allocated to either the DMM surgery (DMM group) or sham surgery (sham group) group. Mice were euthanized 6 weeks post-DMM surgery, and the right hind limbs were promptly excised following euthanasia. All animal care and experimental procedures were conducted in strict adherence with the guidelines of the Experimental Animal Management Institution of Shanxi Medical University (Approval No: DW2022063).

2.10. DMM surgery

To induce post-traumatic OA in the DMM subgroups, pentobarbital sodium inhalation anaesthesia was administered before the surgical procedure. The right knee joints of mice were surgically opened, and the medial meniscotibial ligament (MMTL) was severed to induce joint destabilisation as described [32]. After confirming medial meniscal ligament rupture, the joint and surgical incision were meticulously sutured, layer by layer. In the sham group, the knee joint was exposed without severing the MMTL, and the joints were closed with sutures. After surgery, mice were allowed unrestricted movement and provided with ample food and water.

2.11. CT-based microangiography

Six weeks post-DMM surgery, mice were anesthetised via pentobarbital sodium inhalation anaesthesia. Subsequently, the pericardium was exposed for left ventricular puncture, and a slow injection of 100 units/ml of heparinised saline and 4 % paraformaldehyde was administered to fix the systemic microvasculature. After another injection of heparinised saline, a vascular contrast agent (Microfil) was slowly injected to facilitate observations of the blue contrast agent gradually filling the systemic large and microvessels. After euthanasia, the right knee joint was fixed, decalcified, and scanned for the tibial subchondral bone in the medial compartment using a small-animal CT imaging system (Faxitron). The obtained data were imported into Materialise Mimics software (Version 21.0) for an analysis and quantification of the subchondral bone vessel volume/total tissue volume.

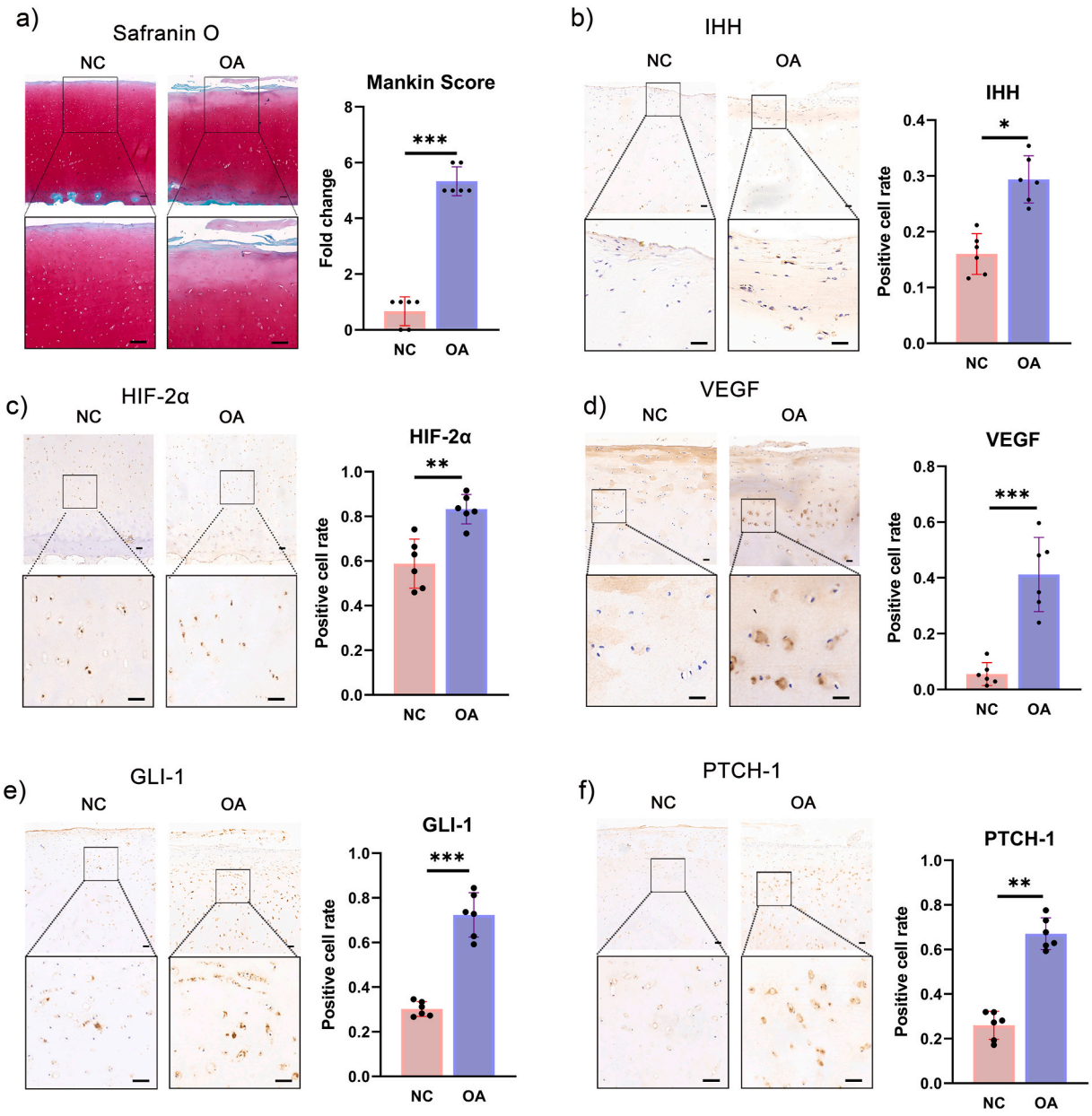

Figure 1. The IHH–GLI-1 pathway exhibits a similar expression trend to HIF-2α and VEGF in early human osteoarthritis (OA) cartilage. a) Safranin O-Fast Green staining of human normal cartilage tissue and early-OA cartilage tissue; according to the staining results, Mankin scoring was performed (n = 6). Scale bar: 50 μm. **b-f)** Immunohistochemical images showing IHH, HIF-2a, VEGF, GLI-1, and PTCH-1 expression in human normal and early-OA cartilage tissues; the average cell positivity was quantified per group (n = 6). Scale bar: 10 μm. The data are presented as the mean ± SD. *ns* $p > 0.05$, *$p < 0.05$, **$p < 0.01$, ***$p < 0.001$. (For interpretation of the references to colour in this figure legend, the reader is referred to the Web version of this article.)

2.12. Micro-CT analysis subchondral bone mierostructure

Six weeks post-DMM surgery, mice were euthanized under inhalation anaesthesia with pentobarbital sodium. The right knee joints were harvested, and the subchondral bone of the medial compartment of the tibia was scanned using a small animal CT imaging system (Faxitron) to perform three-dimensional image reconstruction. Regions of interest (ROI) in the subchondral bone at consistent locations were selected for quantitative analysis of the bone volume fraction (BV/TV), trabecular thickness (Tb.Th), and trabecular number (Tb.N), followed by statistical analysis.

2.13. Statistical analysis

Data were presented as mean ± standard deviation. Statistical evaluation was performed using one-way analysis of variance (ANOVA) for multiple pairwise comparisons, employing the Student-Newman-Keuls method for three or more comparisons; $p < 0.05$ was deemed statistically significant. All statistical analyses were executed using SPSS software for Windows (version 24.0; SPSS Inc., Chicago, IL, USA).

3. Results

3.1. Expression of IHH–GLI-1 pathway components, HIF-2α, and VEGF in early OA

We obtained relatively normal and early degenerated articular cartilage samples from patients undergoing knee joint replacement surgery. Normal cartilage showed a smooth surface, normal hypertrophic chondrocytes, and uniform Safranin O and Alcian blue staining

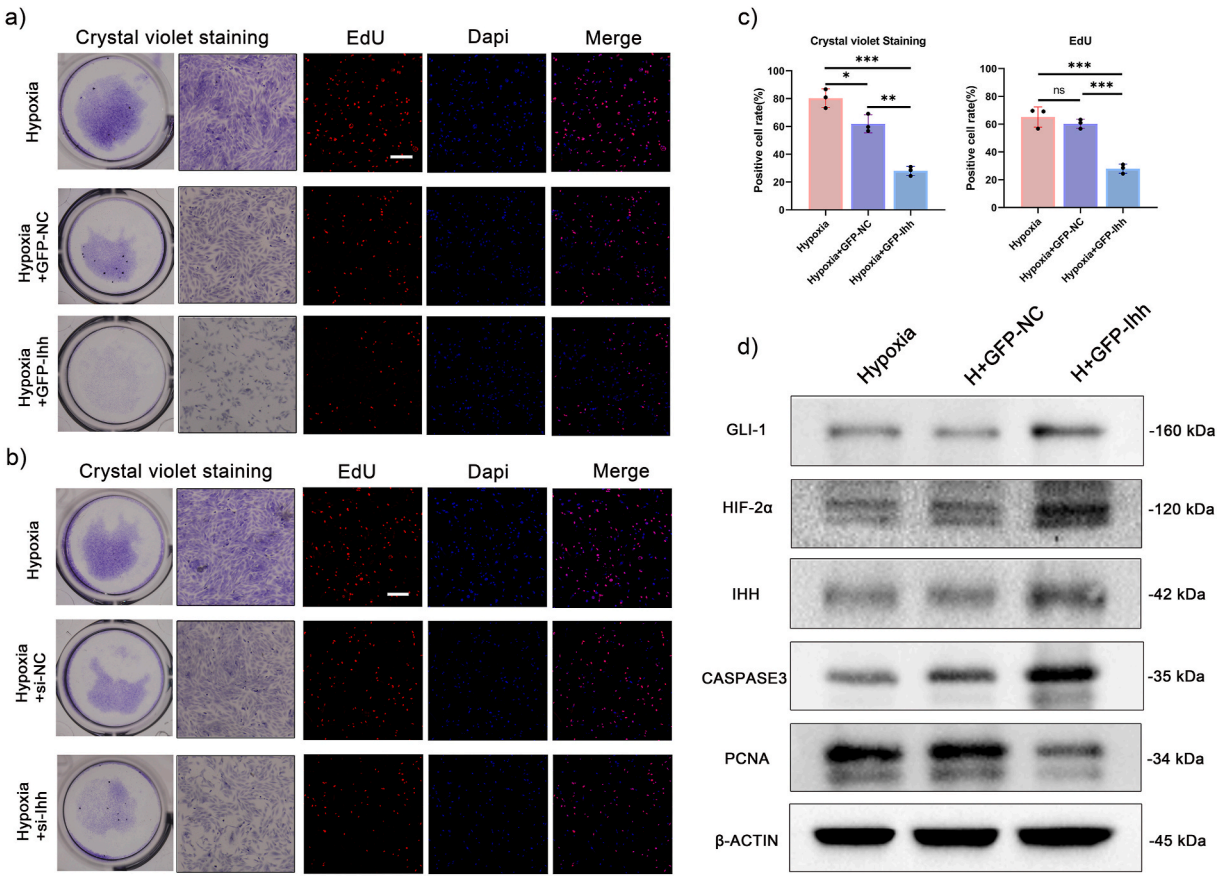

Figure 2. IHH inhibits cell proliferation via HIF-2α in chondrocytes cultured under simulated physiological hypoxic conditions. a) Crystal violet and EdU staining of chondrocytes in GFP-NC and GFP-Ihh groups under hypoxic conditions. Scale bar: 100 μm. **b)** Crystal violet and EdU staining of chondrocytes in si-NC and si-Ihh groups under hypoxic conditions. Scale bar: 100 μm. **c)** Percentage of positive cells based on Crystal violet and EdU staining of chondrocytes in GFP-NC and GFP-Ihh groups under hypoxic conditions. **d)** Western blot analysis of the expression of IHH, GLI-1, HIF-2α, CASPASE3, and PCNA proteins in chondrocytes transfected with GFP-NC and GFP-Ihh after 48 h of hypoxia (n = 3). The data are presented as the mean±SD. *ns* $p > 0.05$, *$p < 0.05$, **$p < 0.01$, ***$p < 0.001$. (For interpretation of the references to colour in this figure legend, the reader is referred to the Web version of this article.)

throughout (Fig. 1a, Fig. S1a). In contrast, early degenerated cartilage was thinner, with an irregular surface, reduced staining, and higher Mankin scores (Fig. 1a). Immunohistochemical staining revealed relatively low IHH expression in the normal cartilage; in early degenerated cartilage, IHH expression was significantly increased and predominantly observed in clusters of damaged chondrocytes in the tangential layer (Fig. 1b). In early degenerated cartilage, HIF-2α expression was elevated in hypertrophic chondrocytes of the radiating and calcification layers (Fig. 1c). VEGF was not expressed in relatively normal cartilage, but its expression significantly increased in early degenerated cartilage, mainly in abnormally hypertrophic chondrocytes of the transitional and radiating layers (Fig. 1d). Meanwhile, GLI-1, PTCH-1, and SMO were expressed in early degenerated cartilage, with significantly increased GLI-1 expression primarily in hypertrophic chondrocytes of the transitional, radiating, and calcification layers (Fig. 1e–f, Fig. S1b). This suggests that IHH might regulate HIF-2α-VEGF expression via the GLI-1 pathway.

3.2. Effects of IHH on chondrocytes in a physiological environment and its relationship with HIF-2α

Chondrocytes under hypoxia were manipulated via IHH overexpression or knockdown. GFP-Ihh and control plasmid transfection was successful, as confirmed by green fluorescence (Fig. S2a). *Ihh* expression increased 2.5-fold in GFP-Ihh-expressing cells, compared to that in normal and GFP-NC cells, and decreased by 70 % with si-Ihh (Fig. S2b). IHH overexpression and knockdown under hypoxic conditions inhibited chondrocyte proliferation, as evidenced by crystal violet and EdU staining (Fig. 2a–c; Fig. S2c). Additionally, IHH verexpression increased, whereas knockdown decreased, IHH, GLI-1, and HIF-2α protein expression (Fig. 2d; Fig. S2d; Figs. S3a–b). Meanwhile, PCNA expression was decreased, indicating reduced proliferation, and CASPASE3 expression was increased, suggesting increased apoptosis (Fig. 2d; Fig. S2d; Figs. S3a–b). These findings suggest that the effect of IHH on chondrocyte proliferation and apoptosis under hypoxic conditions might be mediated by activated HIF-2α.

3.3. IHH regulates HIF-2α expression in inflammatory chondrocytes

To investigate the effect of IHH on HIF-2α during inflammation, chondrocytes were transfected with IHH-expression plasmids and cultured under inflammatory conditions. After IL-1β stimulation, *Ihh*, *Gli-1*, *Vegf*, *Mmp13*, and *Col-X* expression was significantly increased, compared to that in the NC group. IHH overexpression resulted in notably higher *Gli-1*, *Vegf*, *Mmp13*, and *Col-X* expression compared to that in the NC, IL-1β, and IL-1β + GFP-NC groups (Fig. 3a). However, there was no significant difference in *Hif-2α* expression among the groups, indicating that IHH does not affect *Hif-2α* mRNA transcription (Fig. 3a). Western blot analysis after IL-1β stimulation showed increased IHH, HIF-2α, GLI-1, VEGF, MMP13, and COL-X expression compared to that in normal chondrocytes. GFP-Ihh plasmid transfection followed by IL-1β stimulation further elevated this expression (Fig. 3b; Fig. S3c). HIF-2α immunofluorescence staining revealed increased expression after IL-1β stimulation, primarily in the nucleus (Fig. 3c–d; Fig. S3f). IHH

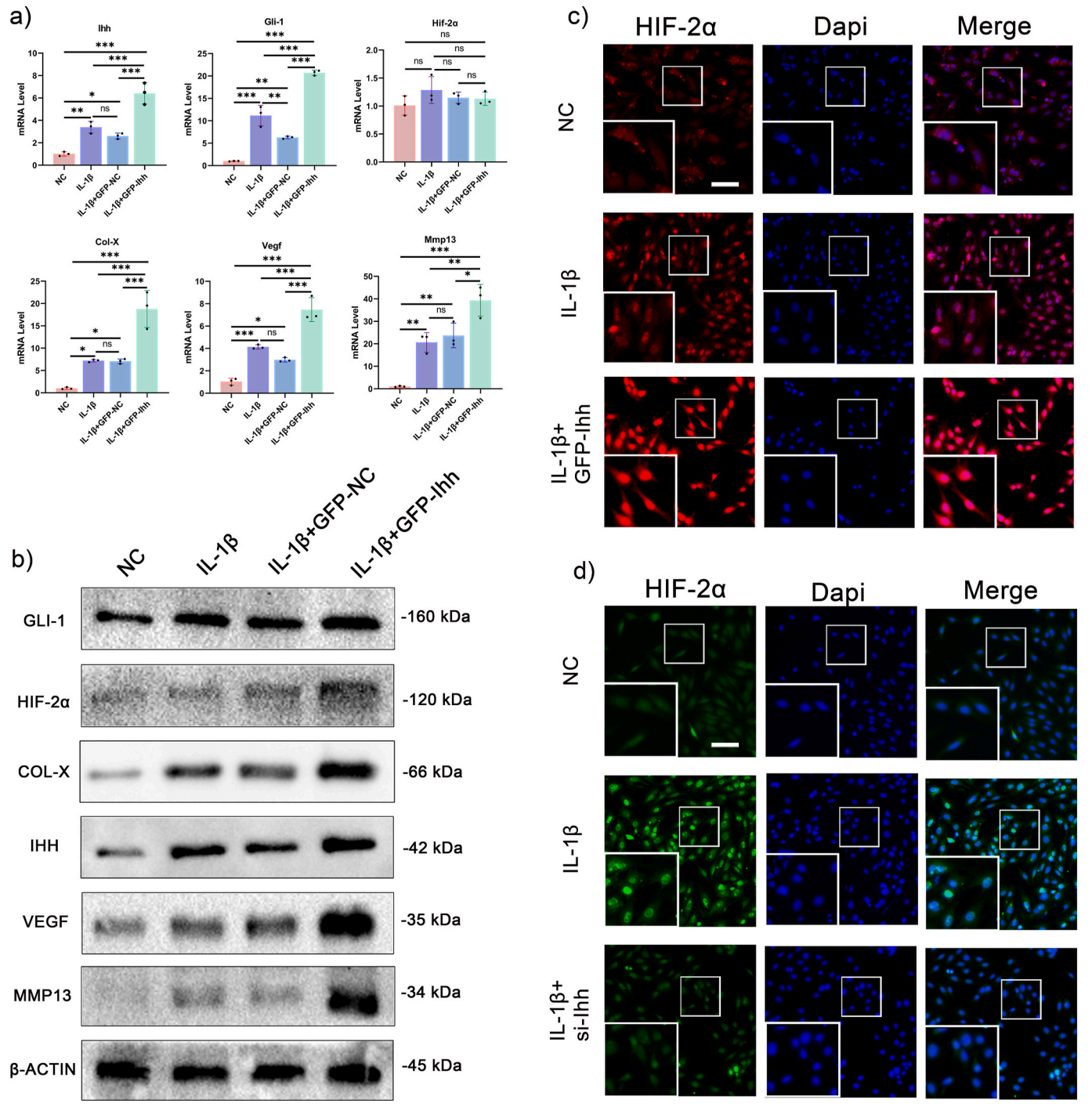

Figure 3. IHH affects HIF-2α expression in inflammation-exposed chondrocytes. a) RT-qPCR was conducted to assess the relative *Ihh*, *Gli-1*, *Hif-2α*, *Col-X*, *Vegf*, and *Mmp13* mRNA expression levels in chondrocytes transfected with GFP-NC and GFP-Ihh under IL-1β-induced inflammatory conditions. Data are shown as normalised fold-expression relative to that in the normal control group (n = 3). **b)** Western blot analysis of the protein expression levels of IHH, GLI-1, HIF-2α, COL-X, VEGF, and MMP13 in chondrocytes transfected with GFP-NC and GFP-Ihh under IL-1β-induced inflammatory conditions (n = 3). **c)** Immunofluorescence images of HIF-2α in chondrocytes transfected with GFP-Ihh under IL-1β-induced inflammatory conditions (n = 3). Immunofluorescence staining of HIF-2α, at 594 nm; DAPI was used to stain cell nuclei. Scale bar, 50 μm. **d)** Immunofluorescence images of HIF-2α in chondrocytes transfected with si-Ihh under IL-1β-induced inflammatory conditions (n = 3). Immunofluorescence staining of HIF-2α, at 488 nm; DAPI was used to stain cell nuclei. Scale bar, 50 μm. The data are presented as that mean ± SD. *ns* $p > 0.05$, **p* < 0.05, ***p* < 0.01, ****p* < 0.001.

overexpression and IL-1β stimulation increased the nuclear fluorescence intensity of HIF-2α, whereas IHH knockdown reduced this (Fig. 3c–d; Fig. S3f). These findings suggest that IHH directly influences HIF-2α protein expression in inflammatory chondrocytes, affecting downstream proteins.

3.4. IHH-GLI-1 and HIF-2α form a positive feedback loop to regulate downstream factors in chondrocytes subjected to inflammation

To elucidate the regulatory interaction between IHH and HIF-2α during inflammation, chondrocytes were transfected with an IHH -overexpression plasmid and exposed to IL-1β to simulate arthritic

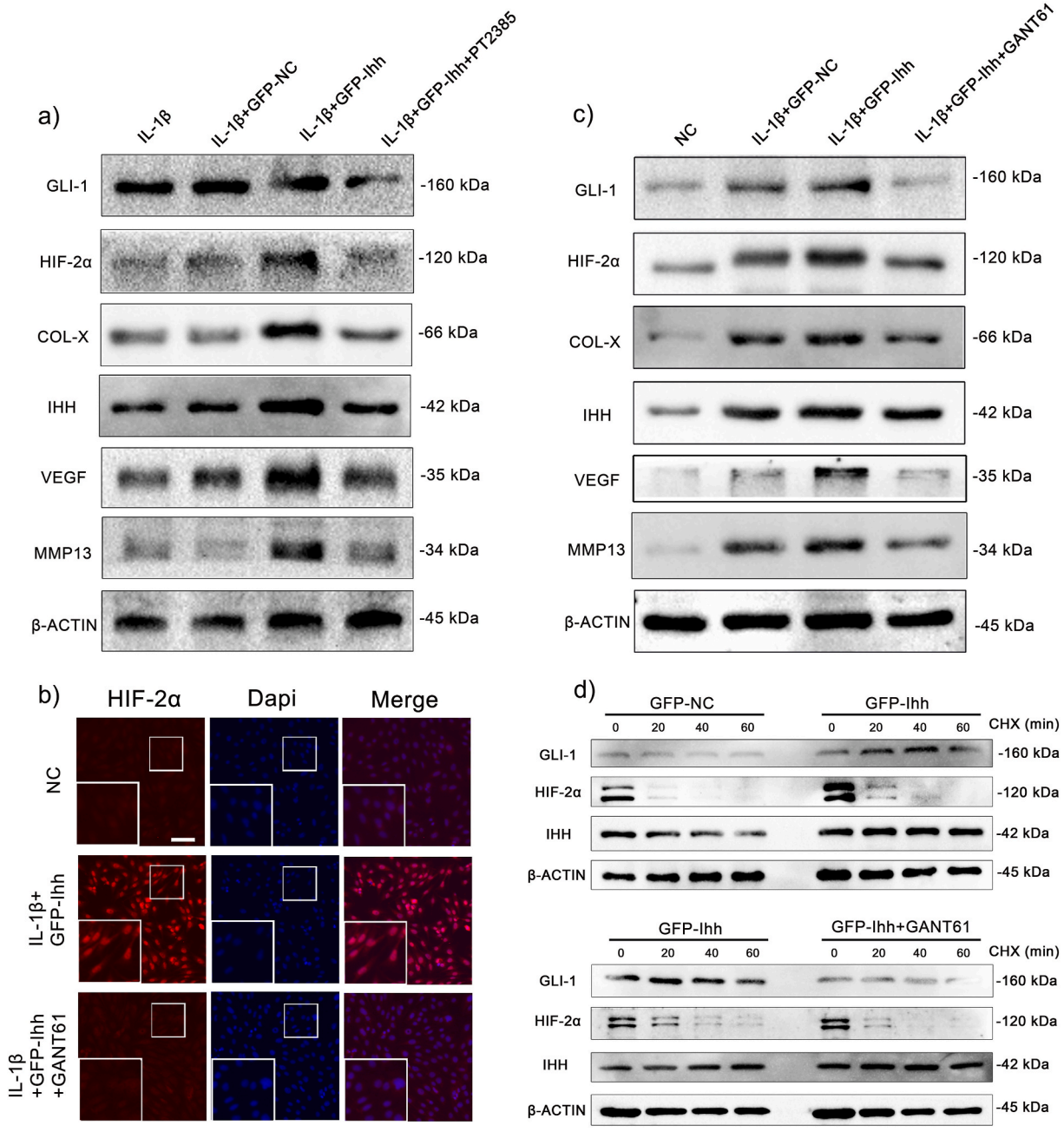

Figure 4. IHH inhibits HIF-2α degradation via GLI-1, promoting a positive IHH–GLI-1 expression feedback loop in inflammation-exposed chondrocytes. a) Western blot analysis of IHH, GLI-1, HIF-2α, COL-X, VEGF, and MMP13 protein expression levels in chondrocytes transfected with GFP-Ihh and simultaneously treated with 20 μM PT2385 under IL-1β-induced inflammatory conditions (n = 3). **b)** Immunofluorescence images of HIF-2α in chondrocytes transfected with GFP-Ihh and simultaneously treated with 100 μM GANT61 under IL-1β-induced inflammatory conditions (n = 3). Immunofluorescence staining of HIF-2α, at 594 nm; DAPI was used to stain cell nuclei. Scale bar, 50 μm. **c)** Western blot analysis of IHH, GLI-1, HIF-2α, COL-X, VEGF and MMP13 protein expression levels in chondrocytes transfected with GFP-Ihh and simultaneously treated with 100 μM GANT61 under IL-1β-induced inflammatory conditions (n = 3). **d)** Western blot analysis of the degradation IHH, GLI-1, and HIF-2α proteins, within 60 min, in chondrocytes transfected with GFP-Ihh and simultaneously treated with 100 μM GANT61 under IL-1β-induced inflammatory conditions (n = 3).

conditions. Subsequently, they were treated with PT2385, a specific HIF-2α inhibitor, for 24 h, and protein levels of HIF-2α and downstream factors were evaluated. Compared to that in the IL-1β and IL-1β+GFP-NC groups, IHH overexpression resulted in a further increase in HIF-2α expression in inflamed chondrocytes, with HIF-2α significantly inhibited following PT2385 treatment (Fig. 4a; Fig. S3d). Concurrently, IHH and GLI-1 expression was markedly decreased, indicating that HIF-2α upregulates IHH and GLI-1 expression in chondrocytes during inflammation (Fig. 4a; Fig. S3d). Additionally, HIF-2α inhibition led to a significant reduction in VEGF, MMP13, and COL-X expression in chondrocytes (Fig. 4a; Fig. S3d). This suggests a positive feedback loop between IHH and HIF-2α, jointly regulating downstream anabolic and catabolic factors.

Next, the role of GLI-1 was investigated using the specific inhibitor GANT61. After 100 μM GANT61 treatment for 24 h, HIF-2α nuclear fluorescence intensity was significantly reduced and weaker than that in the IL-1β and IL-1β+GFP-Ihh groups (Fig. 4b; Fig. S3f). Compared to that in the control group, GLI-1 expression was significantly reduced in chondrocytes treated with GANT61, whereas the expression of HIF-2α and its downstream factors VEGF, MMP13, and COL-X was decreased

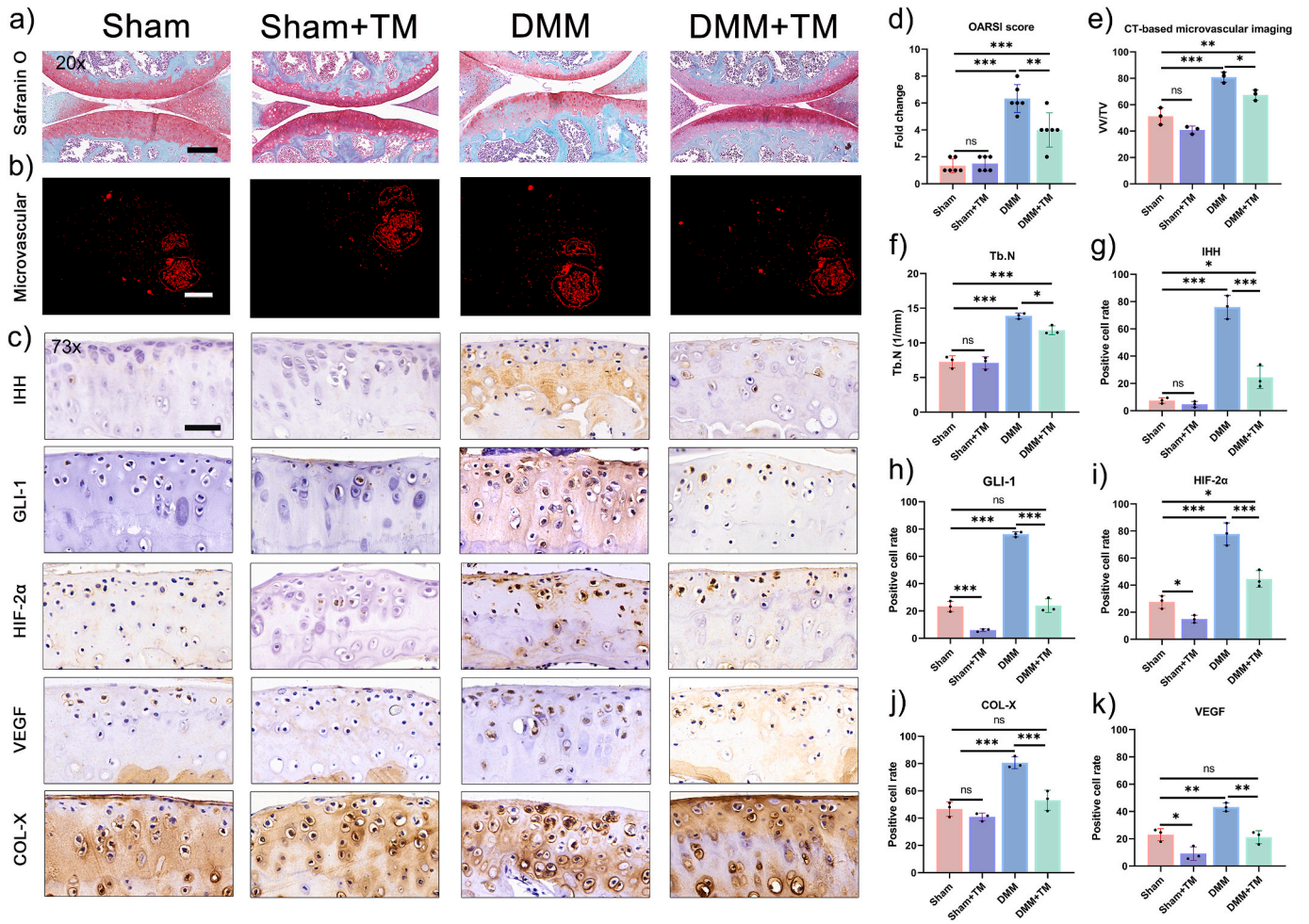

Figure 5. Conditional *Ihh* deletion in early degenerated mouse cartilage disrupts IHH–GLI-1–HIF-2α signalling, delaying osteoarthritis (OA) progression. **a)** Safranin O-Fast Green staining of knee joints from tamoxifen ™-injected Col2a1-Cre^{ERT2}; Ihh$^{fl/fl}$ mice 6 weeks after destabilisation of the medial meniscus (DMM) surgery (n = 6). Scale bar: 200 μm. **b)** Microvascular angiogenesis in the knee joint subchondral bone in TM-injected Col2a1-Cre^{ERT2}; Ihh$^{fl/fl}$ mice 6 weeks after DMM surgery (n = 3). Scale bar: 500 μm. **c)** Immunohistochemical images displaying IHH, GLI-1, HIF-2α, VEGF, and COL-X expression in cartilage from TM-injected Col2a1-Cre^{ERT2}; Ihh$^{fl/fl}$ mice 6 weeks after DMM surgery. Scale bar: 100 μm. **d)** OARSI score for Safranin O-Fast Green staining in TM-injected Col2a1-Cre^{ERT2}; Ihh$^{fl/fl}$ mice 6 weeks after DMM surgery (n = 6). **e)** Quantification the vessel volume relative to the tissue volume (VV/TV) of knee joint subchondral bone in TM-injected Col2a1-Cre^{ERT2}; Ihh$^{fl/fl}$ mice 6 weeks after DMM surgery (n = 3). **f)** Quantification the trabecular numbera (Tb.N) of knee joint subchondral bone in TM-injected Col2a1-Cre^{ERT2}; Ihh$^{fl/fl}$ mice 6 weeks after DMM surgery (n = 3). **g-k)** The average rate of positive cell of immunohistochemical images displaying IHH, GLI-1, HIF-2α, VEGF, and COL-X expression from TM-injected Col2a1-Cre^{ERT2}; Ihh$^{fl/fl}$ mice 6 weeks after DMM surgery (n = 3). The data are presented as the mean ± SD. *ns* $p > 0.05$, *$p < 0.05$, **$p < 0.01$, ***$p < 0.001$. (For interpretation of the references to colour in this figure legend, the reader is referred to the Web version of this article.)

(Fig. 4c; Fig. S3e). Although IHH overexpression initially upregulated the expression of HIF-2α and its downstream factors, this was significantly decreased after GLI-1 inhibition, indicating that IHH regulates HIF-2α expression through the GLI-1 pathway.

CHX was used to further inhibit protein synthesis, and the rate of HIF-2α protein degradation was assessed within 1 h to determine if IHH influences this process through GLI-1. IHH overexpression delayed HIF-2α degradation (Fig. 4d; Fig. S3g). Conversely, following IHH overexpression and subsequent GLI-1 inhibition, the HIF-2α protein degradation rate increased (Fig. 4d; Fig. S3g). These findings imply that IHH influences HIF-2α degradation by inhibiting GLI-1, thus affecting its expression.

3.5. *Ihh* deletion in mouse cartilage affects early cartilage degeneration via HIF-2α

The validated Col2a1-Cre^{ERT2};Ihh$^{fl/fl}$ transgenic mouse model was used to verify the IHH–HIF-2α association during early-onset articular cartilage degeneration. No discernible differences were noted between Col2a1-Cre^{ERT2}; Ihh$^{fl/fl}$ and wild-type mice at 2 months of age. After 1 month of TM injection into Col2a1-Cre^{ERT2}; Ihh$^{fl/fl}$ mice, *Ihh* expression in cartilage tissue decreased by 60 %, with downstream *Gli-1* and *Ptch-1* expression showing reductions of 70 % and 40 %, respectively, indicating successful *Ihh* deletion in chondrocytes (Fig. S4a). Subsequently, destabilisation of the medial meniscus (DMM) surgery was performed. X-ray images revealed bone proliferation and meniscal ossification in both the DMM and DMM + TM groups, indicative of early-stage OA. However, medial joint spaces were narrower the DMM group than in the DMM + TM group, suggesting more severe OA progression in the former (Fig. S4b). Safranin O-fast green staining revealed differences in the cartilage condition among groups. Decreased cartilage matrix thickness, fibrosis, vertical cracks, and weakened safranin O staining were observed in the DMM group, whereas the DMM + TM group had smoother joint surfaces, more uniform safranin O staining, and stronger intensity (Fig. 5a). The OARSI scores confirmed that cartilage degeneration was reduced in the DMM + TM group compared with that in the DMM group (Fig. 5d). Furthermore, knee joint microvasculature CT demonstrated increased subchondral bone microangiogenesis in the

DMM group, which was decreased after *Ihh* deletion in the DMM + TM group, suggesting the inhibition of early subchondral bone layer microvessel generation (Fig. 5b; Fig. 5e). Micro-CT analysis showed that in the DMM group, Tb.N was higher than in the Sham and Sham + TM groups, but significantly decreased after *Ihh* deletion(Fig. 5f). BV/TV and Tb.Th also increased in the DMM group compared to Sham and Sham + TM groups, with no significant changes following *Ihh* deletion (Figs. S4d–e).

We then examined GLI-1 pathway, HIF-2α, and VEGF expression in mouse cartilage tissues. In the DMM group, IHH gene and protein expression were significantly increased. However, in the DMM + TM group, IHH expression was decreased in mid-deep chondrocyte layers (Fig. 5c; Fig. 5g). HIF-2α were expressed in the Sham-group cartilage; however, after *Ihh* deletion, their expression decreased in the Sham + TM group(Fig. 5c; Fig. 5i). In DMM mice, the expression of HIF-2α was significantly increased, whereas in the DMM + TM group, it decreased compared to that in the DMM group but remained higher than that in the Sham and Sham + TM groups (Fig. 5c; Fig. 5i). The expression trends of COL-X, VEGF, and HIF-2α are similar. However, unlike COL-X, VEGF expression is significantly reduced in the Sham + TM group compared to the Sham group after *Ihh* deletion (Fig. 5c; Fig. 5j–k). In normal cartilage, HIF-2α and VEGF were mainly expressed in the superficial and middle layer, with COL-X expression in the deep layer. Post-DMM surgery, their expression increased throughout the layers (Fig. 5c; Fig. 5i–k). *Ihh* deletion led to decreased expression in mid-deep layers, consistent with GLI-1 changes, indicating the role of IHH in accelerating cartilage degeneration primarily in hypertrophic chondrocytes. After *Ihh* deletion, decreased HIF-2α, VEGF, and COL-X expression primarily occurred in the mid-deep pre-hypertrophic and hypertrophic chondrocyte layers, with no significant difference in surface expression changes, consistent with GLI-1 expression changes (Fig. 5c). These results indicate that IHH primarily regulates HIF-2α, VEGF, and COL-X protein expression in hypertrophic chondrocytes, thereby accelerating cartilage degeneration.

4. Discussion

A comparative analysis of early degenerated and relatively normal cartilage tissues revealed elevated expression of IHH and its downstream effectors GLI-1 and PTCH-1 during early cartilage degeneration. Additionally, a notable increase in HIF-2α and downstream VEGF expression was observed. During early degeneration, IHH expression predominantly surged in the tangential layer superficial zone, primarily originating from chondrocytes in this region. This finding aligns with previous research [33], indicating that quiescent chondrocytes in the superficial zone might react to ECM damage as a stress response. Furthermore, the expression of GLI-1 and PTCH-1, downstream of IHH, alongside HIF-2α and downstream VEGF, was upregulated in chondrocytes exhibiting abnormal hypertrophy in the tangential and radiating layers. This suggests potential molecular crosstalk between the IHH pathway and HIF-2α during early joint cartilage degeneration, regulating hypertrophic chondrocyte functions and exacerbating cartilage degeneration.

To investigate the specific mechanism by which IHH regulates HIF-2α, we explored the effects of IHH on HIF-2α in chondrocytes under both physiological and inflammatory conditions and delineated the role of this signalling axis in chondrocyte biology. Under hypoxic conditions, IHH could attenuate chondrocyte proliferation. The discrepancy in findings regarding the influence of IHH expression on chondrocyte proliferation could be attributed to prior research predominantly focusing on reduced chondrocyte proliferation following conditional *Ihh* deletion *in vivo* [34,35]. The literature suggests that HIF-2α, a key member of the hypoxia-inducible factor family, might induce chondrocyte apoptosis [36] with its expression heightened in hypoxic environments. Under hypoxic conditions, IHH impedes chondrocyte proliferation and enhances apoptosis primarily through HIF-2α activation.

In the presence of inflammatory stimuli, IHH does not alter HIF-2α expression in chondrocytes but does affect downstream VEGF expression, suggesting that IHH might modulate HIF-2α expression by directly affecting its protein stability, rather than transcriptional or translational processes. Furthermore, in chondrocytes overexpressing IHH under inflammatory conditions, simultaneous HIF-2α inhibition was observed; whereas IHH enhanced HIF-2α protein expression, its inhibition also decreased IHH–GLI-1 protein expression. These findings corroborate previous research conclusions and collectively suggest a positive feedback loop between IHH–GLI-1 and HIF-2α [10]. In this loop, IHH–GLI-1 promotes HIF-2α protein expression, increases HIF-2α levels, and in turn, augments the IHH–GLI-1 content, exacerbating chondrocyte hypertrophy and promoting surrounding matrix degradation.

GLI-1 inhibition, with GANT61, resulted in reduced expression of HIF-2α and downstream VEGF. Additionally, the similar expression patterns of GLI-1 and HIF-2α *in vivo* confirm that GLI-1 is a direct regulator of HIF-2α and suggest that the effect of IHH on HIF-2α expression is mediated by GLI-1. Whereas IHH did not appear to influence HIF-2α transcriptional processes, the inhibition of protein synthesis in chondrocytes, via CHX, following IHH overexpression significantly slowed HIF-2α degradation. Subsequent GLI-1 inhibition restored the normal HIF-2α degradation rate, demonstrating that IHH–GLI-1 promotes HIF-2α protein expression by inhibiting its degradation.

To validate the associated signalling axis *in vivo*, transgenic mice with a conditional *Ihh* deletion in chondrocytes were generated, and DMM surgery was performed to mimic the effect of IHH on early joint cartilage degeneration. Conditional deletion in mouse cartilage was confirmed to delay early cartilage degeneration [28,37]. Targeting IHH overexpression in early OA through gene interference might thus be an effective strategy for intervention. Following *Ihh* deletion, no significant change in *Hif-2α* expression was observed at the gene level, but at the protein level, HIF-2α and its downstream targets, such as VEGF, were decreased significantly, primarily in hypertrophic chondrocytes. VEGF is a major pro-angiogenic factor, and IHH regulates VEGF expression in the growth plate, thereby promoting endochondral ossification and angiogenesis [38]. However, this function has not been confirmed in OA. In most cases, hedgehog signalling does not directly affect VEGF-mediated angiogenesis, but in certain specific circumstances, it can upregulate VEGF expression to regulate angiogenesis [39]. Our study shows that an *Ihh* deletion reduces HIF-2α and VEGF expression, bridging hedgehog signalling with VEGF, to promote angiogenesis during early cartilage degeneration. The reduction in subchondral bone microvascularization resulting from *Ihh* deletion was accompanied by a decrease in trabecular number. This indicates that Ihh knockout influences the subchondral bone sclerosis process during OA progression. As the samples were collected early after DMM surgery, no significant effects of *Ihh* deletion on BV/TV and Tb.Th were observed, highlighting the need for further research. Moreover, the decreased COL-X expression suggests that IHH influences hypertrophic chondrocyte functions and microvasculature infiltration, potentially via HIF-2α and VEGF regulation, along with factors involved in degradative metabolism.

5. Conclusion

This study clarifies the role of IHH in early cartilage degeneration and provides initial insights into how IHH–GLI-1 affects HIF-2α and downstream factors, demonstrated through *in vivo* experiments. In inflammatory environments affecting chondrocytes, IHH has an inhibitory effect on HIF-2α degradation via the GLI-1 pathway, consequently promoting the expression of HIF-2α and its downstream factors, including VEGF and matrix-degradation factors. Elevated HIF-2α levels can further enhance intracellular IHH–GLI-1 protein contents. Under physiological hypoxic conditions, the IHH–GLI-1–HIF-2α axis in chondrocytes restrains chondrocyte proliferation. Throughout OA progression, this axis predominantly operates within hypertrophic chondrocytes,

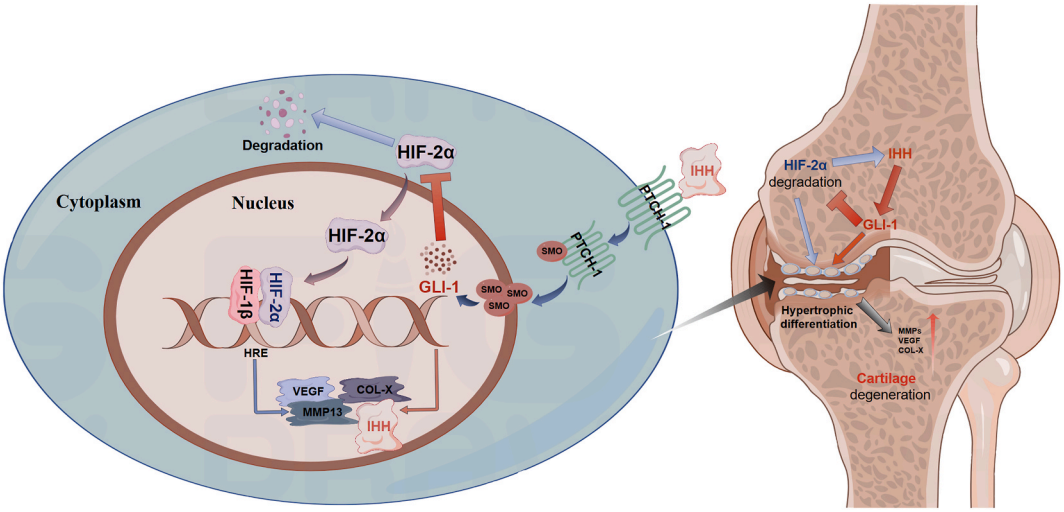

Figure 6. In early-osteoarthritis (OA) chondrocytes, IHH inhibits the degradation of HIF-2α protein through the GLI-1 pathway. Moreover, the elevated expression of HIF-2α amplifies IHH–GLI-1 levels, creating a positive feedback loop. This signalling cascade enhances the expression of downstream hypertrophic factors and matrix-degrading factors, thus worsening cartilage degeneration..

orchestrating processes such as hypertrophic chondrocyte functions, cartilage matrix degradation, and microvascular invasion, thus exacerbating cartilage degeneration. Inhibiting IHH in hypertrophic chondrocytes could disrupt this signalling axis, reducing GLI-1 and HIF-2α expression, and consequently slowing articular cartilage degeneration (Fig. 6).

Declaration of competing interest

The authors declare that they have no known competing financial interests or personal relationships that could have appeared to influence the work reported in this paper.

Acknowledgements

This work was supported by the National Natural Science Foundation of China (Grant No. 82172503, U21A20353, U23A6009), Natural Science foundation of Shanxi Province, China (Grant No. 202203021211035), the Key Medical Research Projects of Shanxi Province, China (Grant No. 2022XM03). We would like to thank Editage (www.editage.cn) for English language editing.

Appendix A. Supplementary data

Supplementary data to this article can be found online at https://doi.org/10.1016/j.jot.2024.09.008.

References

[1] Hunter DJ, Bierma-Zeinstra S. Osteoarthritis. Lancet 2019;393:1745–59.
[2] Dreier R. Hypertrophic differentiation of chondrocytes in osteoarthritis: the developmental aspect of degenerative joint disorders. Arthritis Res Ther 2010;12:216.
[3] Pitsillides AA, Beier F. Cartilage biology in osteoarthritis–lessons from developmental biology. Nat Rev Rheumatol 2011;7:654–63.
[4] Chawla S, Mainardi A, Majumder N, Dönges L, Kumar B, Occhetta P, et al. Chondrocyte hypertrophy in osteoarthritis: mechanistic studies and models for the identification of new therapeutic strategies. Cells 2022;11:4034.
[5] Chawla S, Mainardi A, Majumder N, Dönges L, Kumar B, Occhetta P, et al. Chondrocyte hypertrophy in osteoarthritis: mechanistic studies and models for the identification of new therapeutic strategies. Cells 2022;11.
[6] Mackie EJ, Ahmed YA, Tatarczuch L, Chen KS, Mirams M. Endochondral ossification: how cartilage is converted into bone in the developing skeleton. Int J Biochem Cell Biol 2008;40:46–62.
[7] Hallett SA, Ono W, Ono N. The hypertrophic chondrocyte: to be or not to be. Histol Histopathol 2021;36:1021–36.
[8] Mueller MB, Tuan RS. Functional characterization of hypertrophy in chondrogenesis of human mesenchymal stem cells. Arthritis Rheum 2008;58:1377–88.
[9] Horner A, Bishop NJ, Bord S, Beeton C, Kelsall AW, Coleman N, et al. Immunolocalisation of vascular endothelial growth factor (VEGF) in human neonatal growth plate cartilage. J Anat 1999;194(Pt 4):519–24.
[10] Saito T, Fukai A, Mabuchi A, Ikeda T, Yano F, Ohba S, et al. Transcriptional regulation of endochondral ossification by HIF-2alpha during skeletal growth and osteoarthritis development. Nat Med 2010;16:678–86.
[11] Majumder N, Ghosh S. Unfolding the mystery behind the onset of chondrocyte hypertrophy during chondrogenesis: toward designing advanced permanent cartilage-mimetic biomaterials. Adv Funct Mater 2023;33:2300651.
[12] Ortega N, Behonick DJ, Werb Z. Matrix remodeling during endochondral ossification. Trends Cell Biol 2004;14:86–93.
[13] Alman BA. The role of hedgehog signalling in skeletal health and disease. Nat Rev Rheumatol 2015;11:552–60.
[14] Wei F, Zhou J, Wei X, Zhang J, Fleming BC, Terek R, et al. Activation of Indian hedgehog promotes chondrocyte hypertrophy and upregulation of MMP-13 in human osteoarthritic cartilage. Osteoarthritis Cartilage 2012;20:755–63.
[15] Guo L, Wei X, Zhang Z, Wang X, Wang C, Li P, et al. Ipriflavone attenuates the degeneration of cartilage by blocking the Indian hedgehog pathway. Arthritis Res Ther 2019;21:109.
[16] Liu Q, Wu Z, Hu D, Zhang L, Wang L, Liu G. Low dose of indomethacin and Hedgehog signaling inhibitor administration synergistically attenuates cartilage damage in osteoarthritis by controlling chondrocytes pyroptosis. Gene 2019;712:143959.
[17] Gambassi S, Geminiani M, Thorpe SD, Bernardini G, Millucci L, Braconi D, et al. Smoothened-antagonists reverse homogentisic acid-induced alterations of Hedgehog signaling and primary cilium length in alkaptonuria. J Cell Physiol 2017;232:3103–11.
[18] Bao J, Ma C, Ran J, Xiong Y, Yan S, Wu L. Wnt/β-catenin and Hedgehog pathways are involved in the inflammatory effect of Interleukin 18 on rat chondrocytes. Oncotarget 2017;8:109962–72.
[19] Feng M, Liu W, Ding J, Qiu Y, Chen Q. Sonic hedgehog induces mesenchymal stromal cell senescence-associated secretory phenotype and chondrocyte apoptosis in human osteoarthritic cartilage. Front Cell Dev Biol 2021;9:716610.
[20] Xia L, Zhang HX, Xing ML, Xu YB, Li P, Huang LK, et al. Knockdown of PRMT1 suppresses IL-1β-induced cartilage degradation and inflammatory responses in human chondrocytes through Gli1-mediated Hedgehog signaling pathway. Mol Cell Biochem 2018;438:17–24.
[21] Kimura H, Ng JM, Curran T. Transient inhibition of the Hedgehog pathway in young mice causes permanent defects in bone structure. Cancer Cell 2008;13:249–60.
[22] Hochberg MC, Yerges-Armstrong L, Yau M, Mitchell BD. Genetic epidemiology of osteoarthritis: recent developments and future directions. Curr Opin Rheumatol 2013;25:192–7.
[23] Boer CG, Hatzikotoulas K, Southam L, Stefánsdóttir L, Zhang Y, Coutinho de Almeida R, et al. Deciphering osteoarthritis genetics across 826,690 individuals from 9 populations. Cell 2021;184:6003–5.
[24] Murphy CL. HIF-2alpha–a mediator of osteoarthritis? Cell Res 2010;20:977–9.
[25] Saito T, Kawaguchi H. HIF-2α as a possible therapeutic target of osteoarthritis. Osteoarthritis Cartilage 2010;18:1552–6.
[26] Wu D, Potluri N, Lu J, Kim Y, Rastinejad F. Structural integration in hypoxia-inducible factors. Nature 2015;524:303–8.
[27] Pfander D, Swoboda B, Kirsch T. Expression of early and late differentiation markers (proliferating cell nuclear antigen, syndecan-3, annexin VI, and alkaline

phosphatase) by human osteoarthritic chondrocytes. Am J Pathol 2001;159:1777–83.
[28] Zhou J, Chen Q, Lanske B, Fleming BC, Terek R, Wei X, et al. Disrupting the Indian hedgehog signaling pathway in vivo attenuates surgically induced osteoarthritis progression in Col2a1-CreERT2; Ihhfl/fl mice. Arthritis Res Ther 2014;16:R11.
[29] Maeda Y, Nakamura E, Nguyen MT, Suva LJ, Swain FL, Razzaque MS, et al. Indian Hedgehog produced by postnatal chondrocytes is essential for maintaining a growth plate and trabecular bone. Proc Natl Acad Sci U S A 2007;104:6382–7.
[30] Mankin HJ, Dorfman H, Lippiello L, Zarins A. Biochemical and metabolic abnormalities in articular cartilage from osteo-arthritic human hips. II. Correlation of morphology with biochemical and metabolic data. J Bone Joint Surg Am 1971;53:523–37.
[31] Glasson SS, Chambers MG, Van Den Berg WB, Little CB. The OARSI histopathology initiative - recommendations for histological assessments of osteoarthritis in the mouse. Osteoarthritis Cartilage 2010;18(Suppl 3):S17–23.
[32] Glasson SS, Blanchet TJ, Morris EA. The surgical destabilization of the medial meniscus (DMM) model of osteoarthritis in the 129/SvEv mouse. Osteoarthritis Cartilage 2007;15:1061–9.
[33] Zhang C, Wei X, Chen C, Cao K, Li Y, Jiao Q, et al. Indian hedgehog in synovial fluid is a novel marker for early cartilage lesions in human knee joint. Int J Mol Sci 2014;15:7250–65.
[34] St-Jacques B, Hammerschmidt M, McMahon AP. Indian hedgehog signaling regulates proliferation and differentiation of chondrocytes and is essential for bone formation. Genes Dev 1999;13:2072–86.
[35] Long F, Zhang XM, Karp S, Yang Y, McMahon AP. Genetic manipulation of hedgehog signaling in the endochondral skeleton reveals a direct role in the regulation of chondrocyte proliferation. Development 2001;128:5099–108.
[36] Ryu JH, Shin Y, Huh YH, Yang S, Chun CH, Chun JS. Hypoxia-inducible factor-2α regulates Fas-mediated chondrocyte apoptosis during osteoarthritic cartilage destruction. Cell Death Differ 2012;19:440–50.
[37] Lin AC, Seeto BL, Bartoszko JM, Khoury MA, Whetstone H, Ho L, et al. Modulating hedgehog signaling can attenuate the severity of osteoarthritis. Nat Med 2009;15:1421–5.
[38] Duan X, Murata Y, Liu Y, Nicolae C, Olsen BR, Berendsen AD. Vegfa regulates perichondrial vascularity and osteoblast differentiation in bone development. Development 2015;142:1984–91.
[39] Vokes SA, Yatskievych TA, Heimark RL, McMahon J, McMahon AP, Antin PB, et al. Hedgehog signaling is essential for endothelial tube formation during vasculogenesis. Development 2004;131:4371–80.